Supporting Information

Meziane-Cherif et al. 10.1073/pnas.1402259111

SI Materials and Methods

Cloning and Mutagenesis. Total DNA from enterococci was prepared as previously described (1). Full-length *vanXY* genes were amplified by PCR with oligonucleotide primers that introduced flanking 5′-NdeI and 3′-HindIII sites that were used to clone the gene into p15TV-LIC vector (2), which codes for an N-terminal His_6-tagged protein, followed by a tobacco etch virus (TEV) protease cleavage site and the VanXY ORFs. Mutations in VanXY enzymes were introduced using the QuikChange mutagenesis kit (Stratagene) with oligonucleotide pairs (Table S4).

Protein Expression and Purification. Freshly transformed *Escherichia coli* BL21-CodonPlus (DE3)-RIPL cells were grown in 0.5 L of LB medium containing 100 μg/mL ampicillin. Cultures were grown at 37 °C to an OD_{600} of 0.8 and induced for 16 h at 16 °C with 1 mM isopropyl-1-thio-β-D-galactopyranoside, and cells were then harvested by centrifugation and resuspended in 20 mL of buffer A [50 mM Hepes (pH 7.5), 300 mM NaCl, 10% (vol/vol) glycerol] supplemented with 10% (vol/vol) BugBuster 10X Protein Extraction Reagent (Novagen), 25 units of Benzonase (Sigma-Aldrich), and 5 mM imidazole. The mixture was stirred for 10 min at room temperature and centrifuged at 20,000 × *g* for 45 min, and the supernatant was applied to a 1-mL HisTrap Fast Flow column (GE Healthcare) equilibrated with buffer A containing 40 mM imidazole. The protein was eluted with buffer A with a gradient of 40–500 mM imidazole over 20 mL. Fractions containing the recombinant His-tagged proteins were identified by SDS/PAGE, pooled, and dialyzed overnight against 3 L of 50 mM Hepes (pH 7.5), 300 mM NaCl, 5% (vol/vol) glycerol, 1 mM Tris(2-carboxyethyl)phosphine hydrochloride (TCEP), concentrated when needed with a Centriprep 30 concentrator, and stored at −80 °C. For crystallization of $VanXY_G$, the His_6-tags were cleaved by TEV protease in 500 mM NaCl, 50 mM Tris (pH 7.5), 1 mM TCEP, 1 mM EDTA, and 20% glycerol. Molecular weights in solution were verified by size-exclusion chromatography using a HiLoad 16/60 Superdex 75 size-exclusion column (GE Healthcare).

Crystallization and Structure Determination. Crystals of apo $VanXY_G$ were grown at 23 °C using hanging-drop vapor diffusion by mixing 56 mg/mL protein with reservoir solution containing 0.2 M ammonium sulfate, 0.1 M sodium cacodylate (pH 6.3), and 30% (vol/vol) polyethylene glycol (PEG) 8K. Crystals of apo $VanXY_C^{D59S}$ were grown at 23 °C using hanging-drop vapor diffusion by mixing 10 mg/mL protein with reservoir solution containing 0.1 M magnesium chloride, 0.05 M Mes (pH 5.6), 20% (vol/vol) PEG 8K. Crystals of the $VanXY_G$–PHY and $VanXY_C^{D59S}$–PHY complexes were obtained by first growing crystals of the respective apo-proteins and then transferring to a soaking solution containing reservoir solution supplemented with 75 mM and 50 mM PHY, respectively. PHY, obtained from M. Anderluh and S. Gobec (University of Ljubljana, Ljubljana, Slovenia) was from a racemic mixture of (L, L), (D, L), (L, D), and (D, D) diastereoisomers. Crystals of the $VanXY_C^{D59S}$-D-Ala complex were obtained by cocrystallization from the same reservoir solution as the apo-protein plus 2.5 mM acetyl-L-Lys-D-Ala-D-Ala (Sigma-Aldrich). Crystals of the $VanXY_C^{D59S}$-Cu^{2+}-D-Ala-D-Ala complex were obtained with the following procedure: $VanXY_C^{D59S}$ (apo) was crystallized as above and 0.1 M phenanthroline was added to the crystal drop with a 2-h incubation, followed by transfer of the crystal to a new drop containing reservoir solution [containing 22% (vol/vol) PEG 8K and supplemented with 10 mM $CuCl_2$] for 1.5 h, followed by transfer of the crystal to a final drop (with 1 mM $CuCl_2$ and 20 mM D-Ala-D-Ala) and final incubation of 30 min before cryoprotection. All crystals were cryoprotected with paratone oil before diffraction data collection. Diffraction data were collected at 100 K at beamlines 21-ID-D or 21-ID-G at Life Sciences Collaborative Access Team, Advanced Photon Source, at the following wavelengths: 0.97918 Å (selenomethionine peak) for $VanXY_G$ apo, 1.27689 Å (Zn^{2+} peak) for $VanXY_G$–PHY complex, 1.27696 Å (Zn^{2+} peak) for $VanXY_C^{D59S}$ apo, 1.27696 Å (Zn^{2+} peak) for $VanXY_C^{D59S}$–PHY complex, and 0.97856 Å (selenomethionine peak) for $VanXY_C^{D59S}$–D-Ala complex. Diffraction data for $VanXY_C^{D59S}$–D-Ala-D-Ala complex was collected at a home-source Rigaku Micromax-007 HF copper rotating anode fitted with a Rigaku R-AXIS IV++ image plate detector. Diffraction data were reduced with HKL-3000 (3) or XDS (4) and CCP4 Aimless (5). Presence of Zn^{2+} was verified by X-ray fluorescence at LS-CAT beamline 21ID-D. The $VanXY_G$ apo structure was solved by single-wavelength anomalous dispersion phasing using PHENIX.solve (6), which identified all four of the four selenomethionine residues in the primary sequence. The $VanXY_G$ structure was built using PHENIX.autobuild and refined using PHENIX.refine (6). The $VanXY_G$-PHY, $VanXY_C^{D59S}$ apo, $VanXY_C^{D59S}$–PHY complex, and the $VanXY_C^{D59S}$–D-Ala and $VanXY_C^{D59S}$–D-Ala-D-Ala complex structures were solved by molecular replacement using the apo structure of $VanXY_G$ or $VanXY_C^{D59S}$ as a search model in PHENIX.phaser (6) and refined with PHENIX.refine. All residues of each $VanXY_G$ (residues 1–254) and $VanXY_C^{D59S}$ (residues 1–190) were clearly resolved in the electron density. Occupancy of Zn^{2+} ions in all structures was refined. The presence of ligands was validated using omit maps: all atoms of the ligand and zinc atoms were deleted, followed by simulated annealing (Cartesian) using PHENIX.refine with default parameters, followed by model building into residual positive $F_o - F_c$ density. Occupancy values for PHY were refined. B-factors were refined as isotropic for $VanXY_G$ (apo) and $VanXY_C^{D59S}$ (apo), anisotropic for $VanXY_C^{D59S}$-PHY and $VanXY_G$-PHY, isotropic for $VanXY_C^{D59S}$-D-Ala, and isotropic for $VanXY_C^{D59S}$-Cu^{2+}-D-Ala-D-Ala. All inspection of electron density was carried out using Coot (7). All geometries were verified with PHENIX.refine and the Research Collaboratory for Structural Bioinformatics PDB Validation server. Average B-factor and bond angle/bond length rmsd values were calculated using PHENIX.

Sequence and Structural Analysis. Structure superpositions were performed using Mustang (8). Structure similarity searches were performed using the PDBeFold server (9). The buried surface area between protein chains of $VanXY_C^{D59S}$ was calculated using the PDBePISA server (10). Interactions between enzyme and ligand atoms were identified with PDBsum or Coot; hydrogen bonds shown in figures were cutoff at or below 3.50 Å in length. Pockets/binding cavities were identified using the CASTp server (11) with default probe size of 1.4 Å. Modeling of van peptidases with no solved structures was performed using Phyre2 server (12), with VanX enzymes modeled using the structure of VanX (PDB ID code 1R44) (13) as the template; VanXY and VanY enzymes modeled onto structures of $VanXY_G$. Secondary structure elements in Fig. S2 were assigned based on the solved structures of VanX, $VanXY_G$, and $VanXY_C^{D59S}$. The phylogenetic tree of M15 metallopeptidases in Fig. S8 was calculated using MrBayes (14), with an input of the multiple sequence alignment in Fig. S2, corresponding to the

structure superposition calculated by Mustang, followed by manual editing to ensure gaps correlated with secondary structure elements.

Enzyme Kinetics. The method for assaying D,D-dipeptidase and D,D-pentapeptidase activities of VanXY proteins was based on the amino acid oxidase-lactate dehydrogenase coupled assay (15) using a Uvikon UV931 spectrophotometer (Kontron Instruments). The reaction was carried out in 0.1 mL containing 50 mM Hepes (pH 7.5), 0.2 mM NADH, 0.01 μg of lactate dehydrogenase (LDH), 0.03 μg of D-amino acid oxidase (D-AAO), 100 units of catalase at 37 °C, 15 μg of VanXY, and various concentrations of D-Ala-D-Ala and UDP-MurNAc-pentapeptide [D-Ala] substrates. The dipeptides D-Ala-D-ser, D-Ala-L-Ala, L-Ala-L-Ala, and L-Ala-D-Ala (Genscript Corporation) were also tested as substrates or inhibitors. The steady-state kinetic parameters (the mean values of at least three independent measurements) were obtained by fitting experimental data to the Hanes–Woolf equation using the program EnzFitter (Biosoft). For comparison and because $VanXY_G$ is monomeric whereas $VanXY_C$ is a dimer, catalytic constants k_{cat} for $VanXY_C$ mutants were calculated for one monomer. The inhibition assays were performed after incubation of $VanXY_G$ or $VanXY_C$ (0.5 nmol) with PHY concentrations ranging from 0 to 1 mM in Hepes buffer [50 mM (pH 7.5)], and D-Ala-D-Ala (0.01–2 mM). The K_i values were calculated using Enzfitter software (Biosoft) and determined by fitting experimental data to the equations for competitive, noncompetitive, and mixed inhibition models.

1. Le Bouguénec C, de Cespédès G, Horaud T (1990) Presence of chromosomal elements resembling the composite structure Tn3701 in streptococci. *J Bacteriol* 172(2):727–734.
2. Eschenfeldt WH, Lucy S, Millard CS, Joachimiak A, Mark ID (2009) A family of LIC vectors for high-throughput cloning and purification of proteins. *Methods Mol Biol* 498:105–115.
3. Minor W, Cymborowski M, Otwinowski Z, Chruszcz M (2006) HKL-3000: The integration of data reduction and structure solution—from diffraction images to an initial model in minutes. *Acta Crystallogr D Biol Crystallogr* 62(Pt 8):859–866.
4. Kabsch W (2010) XDS. *Acta Crystallogr D Biol Crystallogr* 66(Pt 2):125–132.
5. Evans P (2006) Scaling and assessment of data quality. *Acta Crystallogr D Biol Crystallogr* 62(Pt 1):72–82.
6. Adams PD, et al. (2010) PHENIX: A comprehensive Python-based system for macromolecular structure solution. *Acta Crystallogr D Biol Crystallogr* 66(Pt 2): 213–221.
7. Emsley P, Cowtan K (2004) Coot: Model-building tools for molecular graphics. *Acta Crystallogr D Biol Crystallogr* 60(Pt 12 Pt 1):2126–2132.
8. Konagurthu AS, Whisstock JC, Stuckey PJ, Lesk AM (2006) MUSTANG: A multiple structural alignment algorithm. *Proteins* 64(3):559–574.
9. Krissinel E, Henrick K (2004) Secondary-structure matching (SSM), a new tool for fast protein structure alignment in three dimensions. *Acta Crystallogr D Biol Crystallogr* 60(Pt 12 Pt 1):2256–2268.
10. Krissinel E, Henrick K (2007) Inference of macromolecular assemblies from crystalline state. *J Mol Biol* 372(3):774–797.
11. Dundas J, et al. (2006) CASTp: Computed atlas of surface topography of proteins with structural and topographical mapping of functionally annotated residues. *Nucleic Acids Res* 34(Web Server issue):W116-8.
12. Kelley LA, Sternberg MJE (2009) Protein structure prediction on the Web: A case study using the Phyre server. *Nat Protoc* 4(3):363–371.
13. Bussiere DE, et al. (1998) The structure of VanX reveals a novel amino-dipeptidase involved in mediating transposon-based vancomycin resistance. *Mol Cell* 2(1):75–84.
14. Ronquist F, Huelsenbeck JP (2003) MrBayes 3: Bayesian phylogenetic inference under mixed models. *Bioinformatics* 19(12):1572–1574.
15. Aráoz R, et al. (2000) Mechanism-based inactivation of VanX, a D-alanyl-D-alanine dipeptidase necessary for vancomycin resistance. *Biochemistry* 39(51):15971–15979.

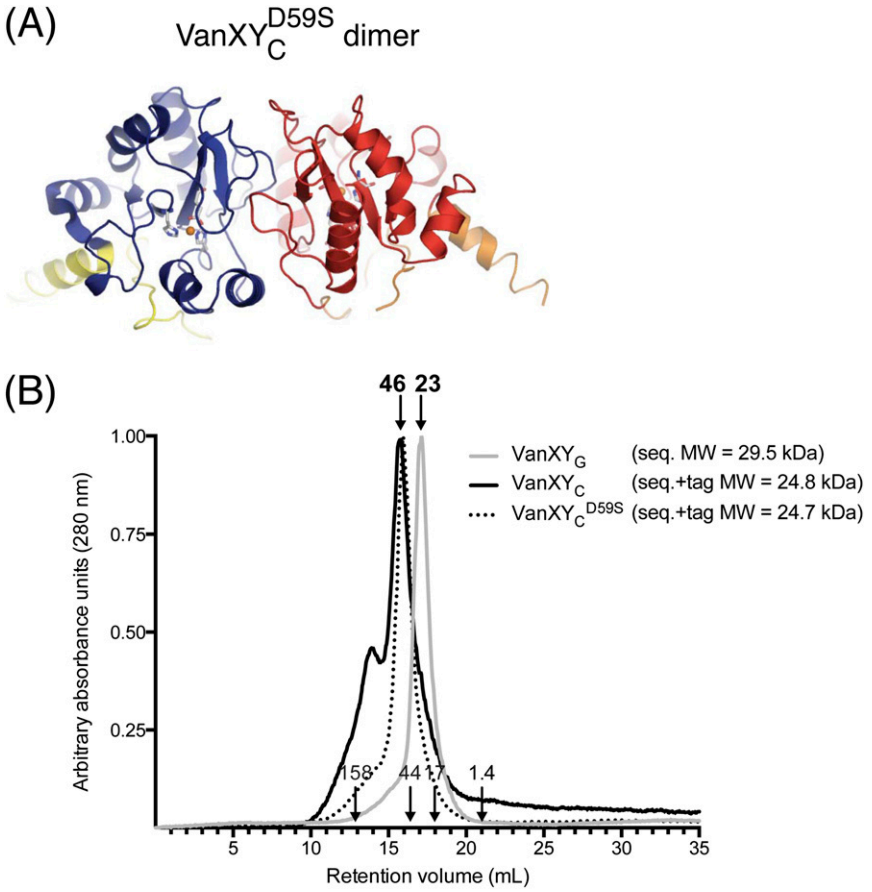

Fig. S1. Oligomeric states of VanXY$_C^{D59S}$ and VanXY$_G$. (*A*) The two chains in the asymmetric unit of the VanXY$_C^{D59S}$ crystal are shown, forming a presumptive dimer. The first chain is colored as in Fig. 1 (residues 1–20 and 175–188 yellow, 21–174 blue); second chain, residues 1–20 and 175–188 orange, 21–174 red. (*B*) Size-exclusion chromatography profiles of VanXY$_C$, VanXY$_C^{D59S}$, and VanXY$_G$. To account for dilution and loading differences, absorbance values (280 nm) were scaled to a common arbitrary scale. Calculated molecular masses in kDa are indicated in bold at the top of the plot, and calibration standards in kDa are indicated at the bottom of the plot. Sequence molecular masses (in some cases containing expression tag) are indicated at the right of the plot.

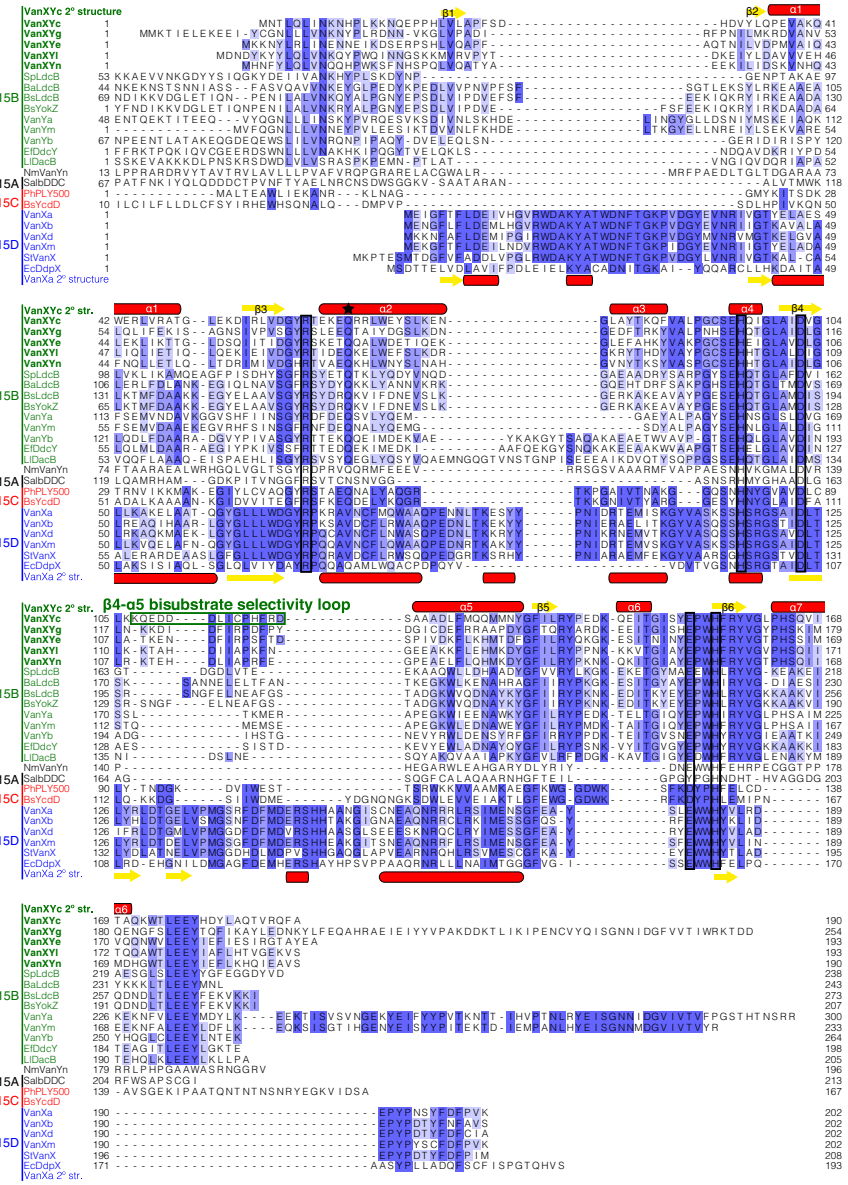

Fig. S2. Structure-based multiple sequence alignment of M15 family peptidases. Sequences are grouped, and their names are colored according to MEROPS subfamilies M15A, M15B, M15C, and M15D. VanXY names are bolded and placed at the top of the alignment. Secondary structure elements (red, helices; yellow, strands) from the crystal structures of $VanXY_C$ and VanX are indicated above and below the alignment, respectively, and labeled for $VanXY_C$. β4–α5 bisubstrate selectivity loop from $VanXY_C$ is boxed in green. Residues essential for catalytic mechanism (His-Asp-His Zn^{2+}-coordinating triad, transition state-stabilizing Arg, and catalytic base Glu) are boxed in black. The glutamine (Gln67 in $VanXY_C$, Gln79 in $VanXY_G$) involved in conferring carboxypeptidase activity is indicated with a black star above the alignment.

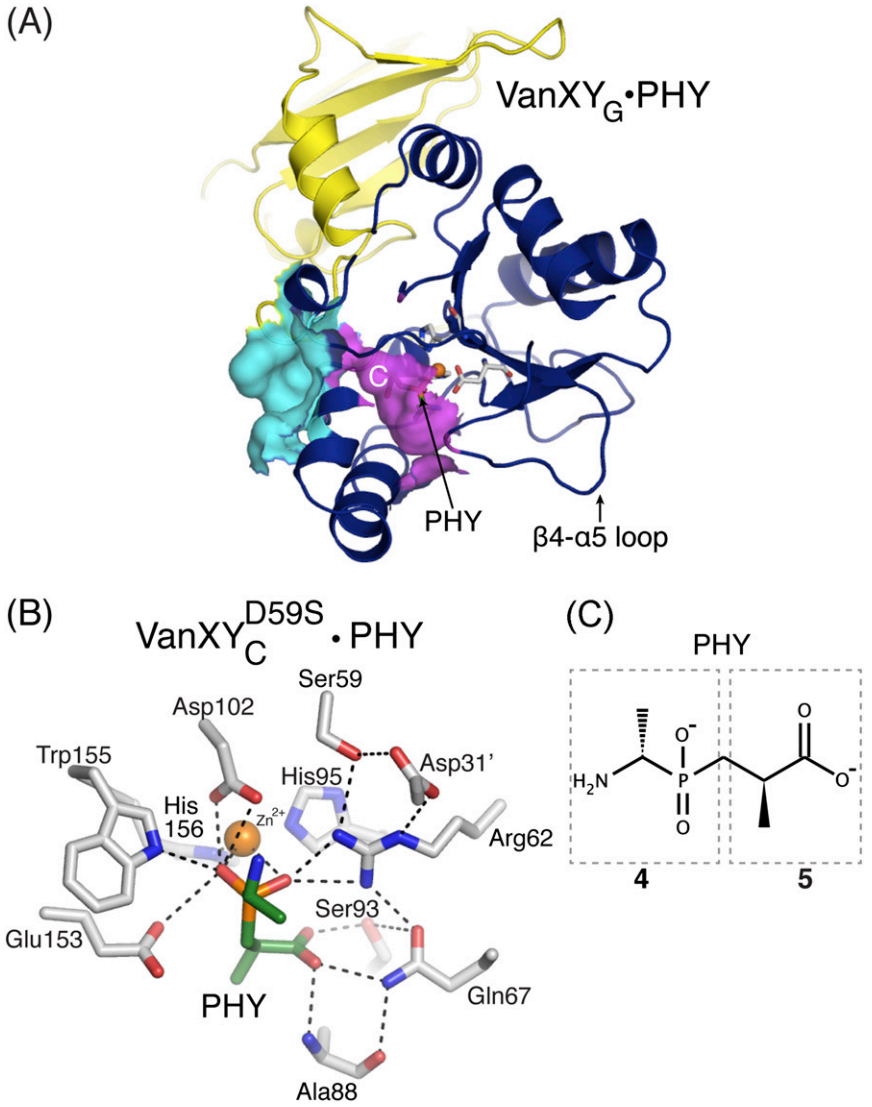

Fig. S3. Structure of VanXY$_C^{D59S}$•PHY complex. (*A*) Overall structure of VanXY$_G$•PHY complex. Surface-exposed surface representation is shown in cyan and purple as in Fig. 2*C*. (*B*) Interactions between VanXY$_C^{D59S}$, Zn^{2+}, and PHY, shown in same view as Fig. 2 *D* and *E*. (*C*) Chemical structure of PHY, phosphinate D-Ala-D-Ala analog, numbered according to the pentapeptide[D-Ala] it mimics, as in Fig. 2*A*.

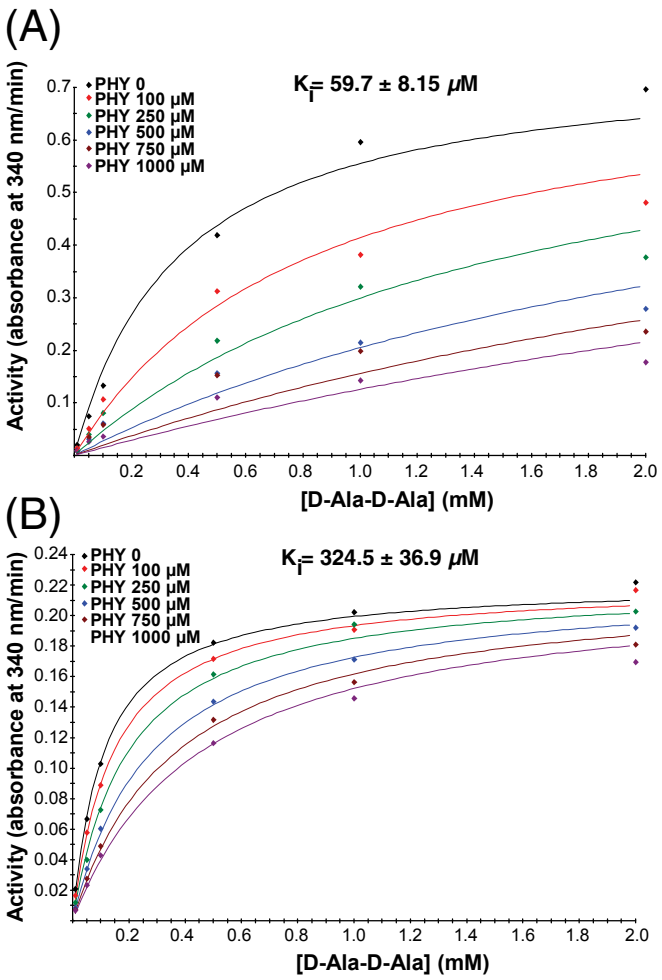

Fig. S4. Inhibition kinetics of PHY against D-Ala-D-Ala hydrolysis by VanXY enzymes. $VanXY_C$ (*A*) and $VanXY_G$ (*B*) activities after addition of enzyme to a mixture of D-Ala-D-Ala (0–2 mM) and PHY at different concentrations (0–1 mM). The Lineweaver–Burk plots at different concentrations of PHY were best-fitted to a competitive inhibition. Apparent K_i values are indicated on each graph and were calculated by using Enzfitter software (Biosoft).

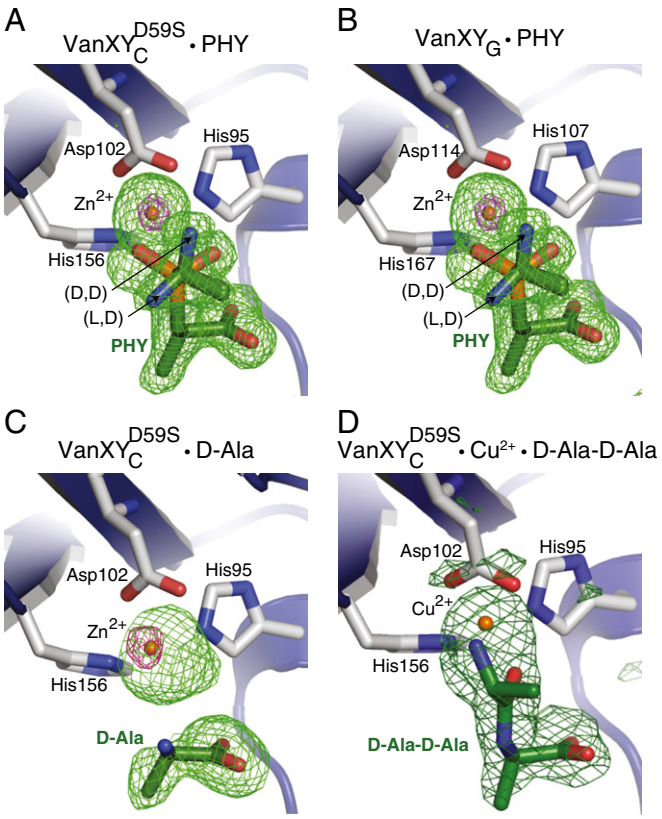

Fig. S5. Electron density of VanXY ligands. Shown is stick representations of PHY bound to active sites of (*A*) VanXY$_C^{D59S}$ and (*B*) VanXY$_G$, (*C*) D-Ala bound to VanXY$_C^{D59S}$, and (*D*) D-Ala-D-Ala bound to VanXY$_C^{D59S}$. Green mesh, simulated annealing omit ($F_o - F_c$) density after omitting ligand atoms at 3 σ. Purple mesh, anomalous difference density at 15 σ (*A* and *B*), and 6 σ (*C*), corresponding to Zn^{2+} ions. Both (L, D) and (D, D) diastereoisomers of PHY are shown and labeled.

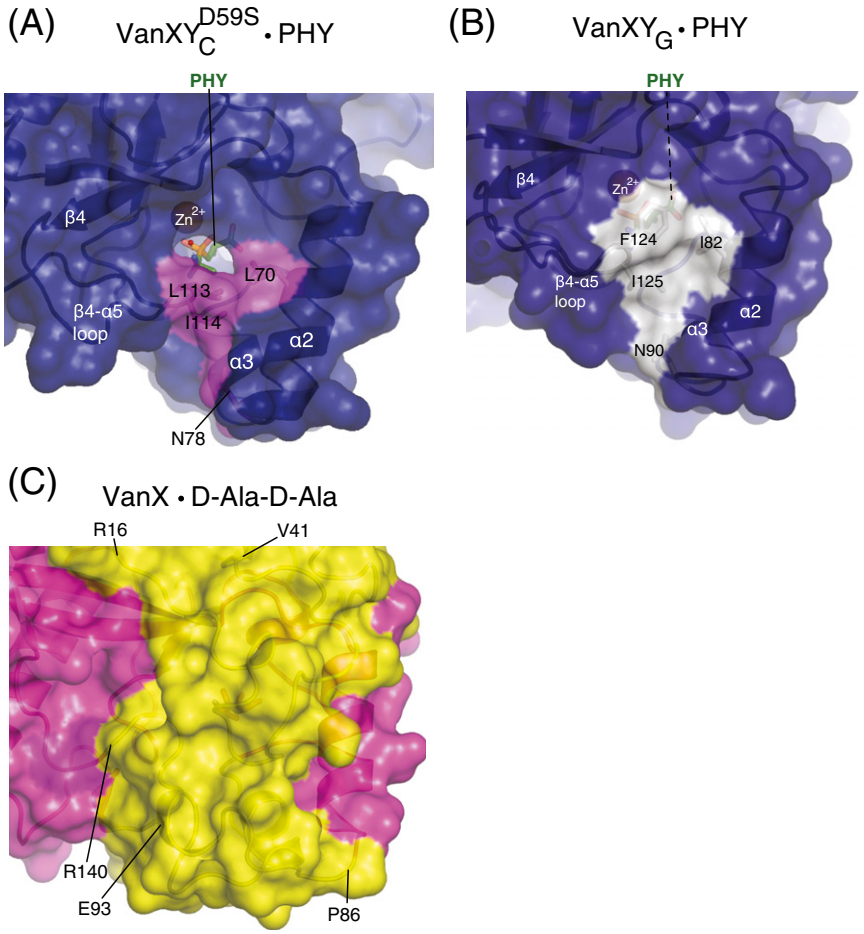

Fig. S6. Putative UDP-MurNAc-L-Ala-D-γ-Glu-L-Lys-D-Ala-D-Ala binding cavity in VanXY$_C$ and equivalent regions of VanXY$_G$ and VanX. (*A*) View of VanXY$_C^{D59S}$ putative UDP-MurNAc-L-Ala-D-γ-Glu-L-Lys-D-Ala-D-Ala binding cavity from the VanXY$_C^{D59S}$-PHY complex. Residues experimentally shown to interact with this substrate are colored in magenta. (*B*) View of VanXY$_G$ showing equivalent view as in *A*. Residues shaded white and labeled are those equivalent to VanXY$_C^{D59S}$ residues shown to interact with UDP-MurNAc-L-Ala-D-γ-Glu-L-Lys-D-Ala-D-Ala. (*C*) View of VanX showing equivalent view as in *A*. Yellow, VanX-specific secondary structures elements, including N-terminal residues that block the presence of the UDP-MurNAc-L-Ala-D-γ-Glu-L-Lys-D-Ala-D-Ala binding cavity (residues within these elements of VanX are labeled).

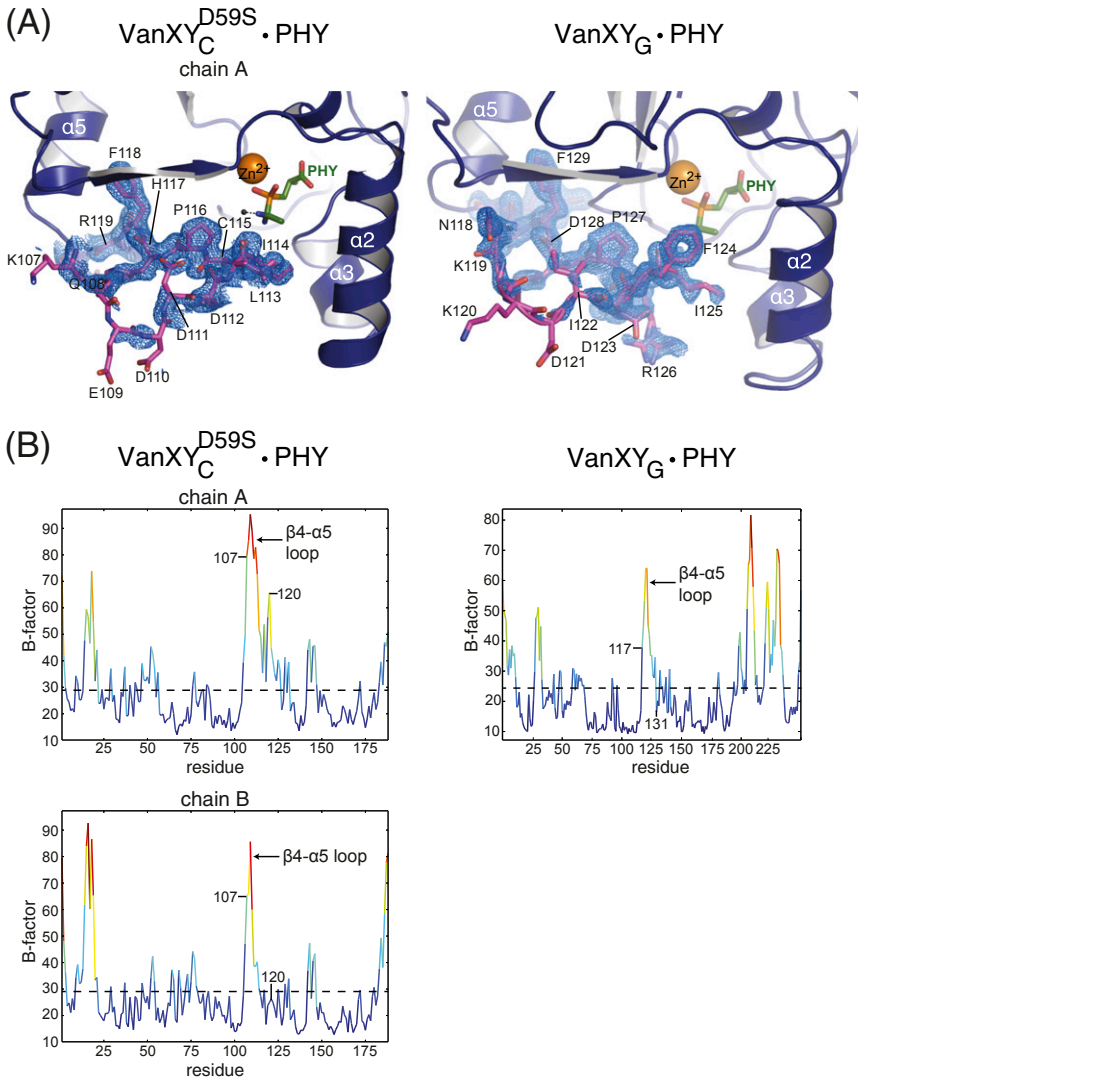

Fig. S7. Electron density and B-factors of bisubstrate selectivity loop (β4–α5) of VanXY enzymes. (*A*) VanXY$_C$ (*Left*) residues in β4–α5 loop are shown in magenta sticks, coordinates obtained from complex structure with PHY. VanXY$_G$ (*Right*) residues in the equivalent region from complex with PHY. Electron density is $2F_O - F_C$ density contoured at 1 σ. (*B*) Average per-residue B-factors as calculated by Phenix for chains A and B of VanXY$_C$ (*Left*) and VanXY$_G$ (*Right*); β4-α5 loop is labeled. Dashed lines, average B-factor for the full-length protein.

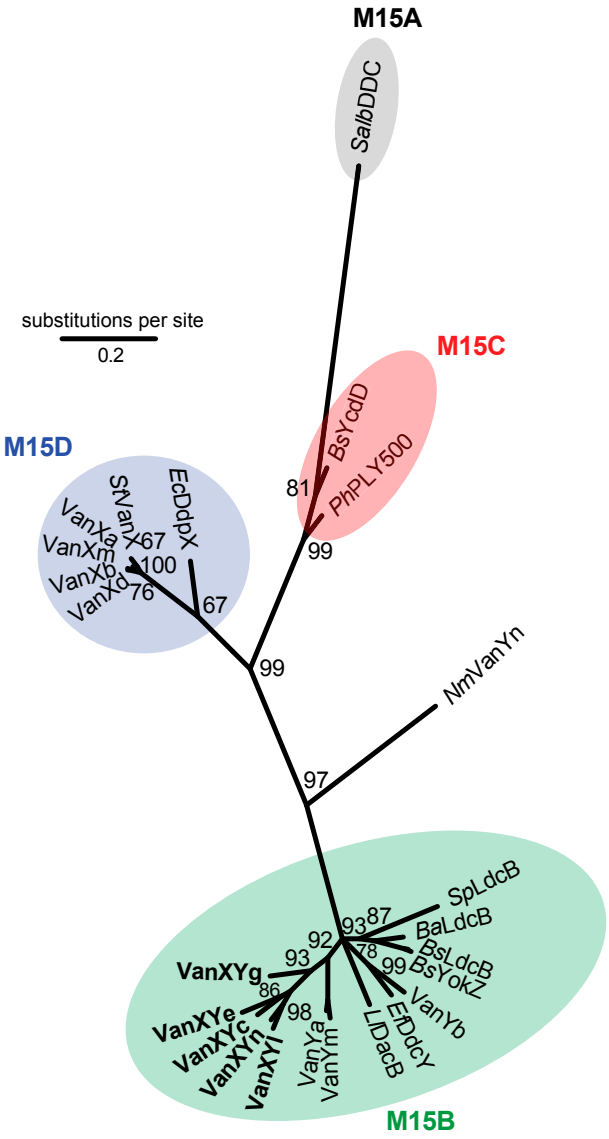

Fig. S8. Phylogenetic reconstruction of metallopeptidase M15 family enzymes. Phylogeny was calculated using MrBayes (14) and the structure-based multiple-sequence alignment in Fig. S2. Sequences are grouped and sequence names are colored according to MEROPS subfamilies M15A, M15B, M15C, and M15D. Bootstrap replicates (out of 100) are labeled at each node. *Ba*, *Bacillus anthracis*; *Bs*, *Bacillus subtilis*; *Ec*, *Escherichia coli*; *Ef*, *Enterococcus faecium*; *Ll*, *Lactococcus lactis*; *Nm*, *Nonomurea* sp. ATCC 39727; *Ph*, bacteriophage A500; *S.alb*, *Streptomyces albus* G; *Sp*, *Streptococcus pneumoniae*; *St*, *Streptomyces toyocayensis*.

Table S1. X-ray diffraction data collection and refinement statistics

	Enzyme / ligand / PDB ID code					
	$VanXY_C^{D59S}$ / N/A / 4MUR	$VanXY_C^{D59S}$ / PHY / 4MUS	$VanXY_C^{D59S}$ / D-Ala / 4MUT	$VanXY_C^{D59S}$ / Cu^{2+}-D-Ala-D-Ala / 4OAK	$VanXY_G$ / N/A / 4F78	$VanXY_G$ / PHY / 4MUQ
Data collection						
Space group	P1	P1	P1	P1	$P2_1$	$P2_1$
Cell dimensions						
a, *b*, *c*, Å	44.2, 44.7, 62.5	44.3, 44.8, 62.4	44.7, 45.2, 63.0	41.9, 43.1, 66.3	38.9, 44.0, 80.2	38.9, 43.7, 80.2
α, β, γ, °	86.3, 77.7, 63.7	86.8, 77.3, 64.2	86.7, 77.2, 63.9	80.5, 74.5, 64.0	90.0, 99.2, 90.0	90.0, 99.2, 90.0
Resolution, Å	40.09–1.63	38.67–1.67	39.13–2.25	19.3–2.0	79.17–1.95	79.20–1.36
R_{merge}*	0.091 (0.512)†	0.086 (0.396)†	0.090 (0.573)†	0.079 (0.518)†	0.078 (0.329)†	0.063 (0.578)†
$I/\sigma(I)$	18.0 (3.4)	19.6 (4.9)	10.3 (2.4)	11.0 (2.3)	10.6 (3.6)	17.2 (3.0)
Completeness, %	96.8 (92.1)	97.3 (94.2)	98.5 (97.7)	94.9 (92.3)	100.0 (100.0)	96.9 (94.2)
Redundancy	7.4 (6.1)	8.1 (4.9)	3.9 (3.9)	3.3 (3.3)	3.3 (3.3)	7.7 (7.6)
Refinement						
Resolution, Å	34.45–1.65	20.0–2.37	34.57–2.25	19.3–2.00	39.6–1.95	23.90–1.98
No. of reflections: working, test‡	46,109, 2,480	67,481, 3,406	20,134, 2,053	25,759, 1,297	35,726, 1,875	111,054, 5,461
R-factor/free	15.7/19.9	16.0/21.5	16.2/18.5	18.9/23.5	15.5/18.6	15.7/21.6
R-factor§	(27.9/34.2)†	(18.8/21.8)†	(27.8/32.3)†	(30.0/37.0)†	(21.7/27.8)†	(25.1/34.0)†
No. of refined atoms (molecules)						
Protein	3,245 (2)	3,186 (2)	3,141 (2)	3,166 (2)	2,095 (1)	2,123 (1)
Zn^{2+}	2	2	2	2¶	1	1
Ligand	N/A	48 (4)¶	15 (2)	22	N/A	24 (2)‖
Solvent	37	28	10	60	64	78
Water	612	530	315	335	191	294
B-factors						
Protein	25.4	29.0	48.0	33.8	25.7	24.0
Zn^{2+}	18.8	16.3	34.3	24.2¶	19.9	10.3
Ligand	N/A	23.5	49.6	35.9	N/A	18.3
Solvent	51.4	35.0	57.1	58.9	43.8	49.4
Water	39.1	40.6	51.3	40.4	31.8	36.1
rmsd						
Bond lengths, Å	0.012	0.007	0.009	0.018	0.016	0.014
Bond angles, °	1.072	1.289	1.129	0.810	1.494	1.397
Ramachandran						
Most favored, %	91.1	91.3	90.7	88.2	86.9	90.1
Additionally fav.	8.9	8.4	9.3	11.5	13.1	9.5
Generously fav.	0	0.3	0	0.3	0	0.5
Disallowed	0	0	0	0	0	0

*$R_{merge} = \Sigma_h\Sigma_i|I_i(h) - \langle I(h)\rangle|/\Sigma_h\Sigma_i I_i(h)$, where $I_i(h)$ and $\langle I(h)\rangle$ are the *i*th and mean measurement of the intensity of reflection *h*.
†Figures in parentheses indicate the values for the outer shells of the data.
‡The number of reflections indicated is the unmerged reflections.
§$R = \Sigma|F_p^{obs} - F_p^{calc}|/\Sigma F_p^{obs}$, where F_p^{obs} and F_p^{calc} are the observed and calculated structure factor amplitudes, respectively.
¶Refers to Cu^{2+} atoms.
‖PHY contains 12 atoms per molecule; two diastereoisomers are observed bound to each chain of each VanXY enzyme.

Table S2. Substrate stereospecificity of $VanXY_C$

Substrate	K_m, mM	k_{cat}, min^{-1}	k_{cat}/K_m, $mM^{-1}\cdot min^{-1}$	Relative k_{cat}/K_m
D-Ala-D-Ala	0.49 ± 0.15	131.7 ± 18.75	268.7	1.00
L-Ala-D-Ala	1.8 ± 0.5	1.25 ± 0.09	0.7	0.003
L-Ala-L-Ala	NA	ND	NA	—
D-Ala-L-Ala	NA	ND	NA	—

NA, Not applicable; ND, not detected.

Table S3. Kinetic characterization of $VanXY_C$ and $VanXY_G$ mutants

	Substrate					
	D-Ala-D-Ala			UDP-MurNAc-L-Ala-D-γ-Glu-L-Lys-D-Ala-D-Ala		
Enzyme	K_m, mM	k_{cat}, min^{-1}	k_{cat}/K_m, $mM^{-1}\cdot min^{-1}$	K_m, mM	k_{cat}, min^{-1}	k_{cat}/K_m, $mM^{-1}\cdot min^{-1}$
$VanXY_C$						
WT	0.49 ± 0.15	131.7 ± 18.75	268.7	1.39 ± 0.12	27.7 ± 1.65	19.9
N8A	0.53 ± 0.07	30.0 ± 1.11	56.7	0.64 ± 0.03	12.5 ± 0.315	19.5
K9F	0.60 ± 0.04	14.7 ± 0.29	24.5	1.60 ± 0.11	18.5 ± 0.63	11.6
D59S	0.31 ± 0.06	14.6 ± 0.75	47.0	0.85 ± 0.26	12.1 ± 2.04	14.2
Q67S	0.61 ± 0.18	29.5 ± 1.87	48.3	1.23 ± 0.24	28.6 ± 3.01	23.3
Q67E	8.57 ± 0.79	18.7 ± 0.57	2.2	0.53 ± 0.2	1.6 ± 0.29	3.0
L70E	35.20 ± 14.10	14.1 ± 2.3	0.4	12.60 ± 9.2	8.2 ± 4.55	0.7
E77L	0.75 ± 0.04	22.1 ± 0.36	29.5	0.22 ± 0.02	4.3 ± 0.15	19.6
N78F	0.29 ± 0.09	35.2 ± 2.37	121.4	0.25 ± 0.11	29.4 ± 4.48	117.6
Y82F	0.74 ± 0.11	32.5 ± 1.4	43.9	0.77 ± 0.1	12.5 ± 0.66	16.2
Y82K	0.68 ± 0.07	30.1 ± 0.9	44.3	0.67 ± 0.08	12.9 ± 0.55	19.3
K84F	0.31 ± 0.04	10.8 ± 0.45	34.7	0.65 ± 0.14	8.4 ± 0.94	12.9
K84E	0.41 ± 0.07	16.0 ± 0.55	39.0	0.32 ± 0.09	7.2 ± 0.79	22.3
A88D	1.28 ± 0.20	5.4 ± 0.28	4.2	13.80 ± 4.5	10.5 ± 2.7	0.8
A88L	0.37 ± 0.02	9.8 ± 0.12	26.5	0.35 ± 0.15	6.8 ± 1.15	19.4
L89F	0.40 ± 0.06	17.1 ± 1.01	42.7	0.83 ± 0.19	14.2 ± 1.8	17.2
L99A	0.45 ± 0.03	19.4 ± 0.57	43.1	0.75 ± 0.16	8.0 ± 0.54	10.7
D111I	0.58 ± 0.03	15.2 ± 0.2	26.2	0.55 ± 0.16	11.9 ± 1.65	21.6
D112L	0.27 ± 0.02	8.4 ± 0.16	31.0	0.56 ± 0.05	9.6 ± 0.45	17.1
L113F	0.16 ± 0.02	26.4 ± 0.6	165.2	0.42 ± 0.05	26.5 ± 4.415	63.0
L113E	0.27 ± 0.05	34.9 ± 1.3	129.1	0.63 ± 0.05	116.4 ± 4.55	184.8
D59S, L113F	0.27 ± 0.06	65.1 ± 2.68	241.1	0.48 ± 0.09	5.3 ± 0.13	11.1
I114E	0.17 ± 0.08	2.7 ± 0.215	15.6	0.58 ± 0.11	59.3 ± 5.48	102.2
C115R	0.45 ± 0.08	109.0 ± 5.86	242.2	2.03 ± 0.72	30.5 ± 2.73	15.0
C115E	0.52 ± 0.02	10.1 ± 0.08	19.4	1.06 ± 0.22	12.2 ± 1.55	11.5
G149L	0.27 ± 0.03	10.4 ± 0.35	38.5	0.60 ± 0.002	9.7 ± 0.02	16.2
G149E	0.47 ± 0.06	23.5 ± 1.35	50.0	0.88 ± 0.05	19.9 ± 0.46	22.6
G149F	0.36 ± 0.03	14.3 ± 0.35	39.7	0.82 ± 0.11	10.2 ± 0.8	12.5
I150G	7.03 ± 1.34	8.7 ± 0.65	1.2	4.50 ± 1.22	2.2 ± 0.3	0.5
I150A	2.77 ± 0.54	12.9 ± 0.72	4.7	2.96 ± 0.33	15.8 ± 1.21	5.3
E153A	NA	ND	NA	NA	ND	NA
Δ106–117	0.87 ± 0.05	12.2 ± 0.2	14.0	1.10 ± 0.27	6.9 ± 0.76	6.2
Δ110–115	0.32 ± 0.12	0.4 ± 0.03	1.1	NA	ND	NA
$VanXY_G$						
WT	0.7 ± 0.21	8.9 ± 0.06	12.7	NA	ND	NA
S71D	0.12 ± 0.02	3.3 ± 0.2	27.5	NA	ND	NA
R74A	NA	ND	NA	NA	ND	NA
R74H	NA	ND	NA	NA	ND	NA
Q79E	NA	ND	NA	NA	ND	NA
Q79S	NA	ND	NA	NA	ND	NA
I82A	0.28 ± 0.03	10.4 ± 0.24	40	NA	ND	NA
F94A	0.54 ± 0.1	12.6 ± 0.53	23.3	NA	ND	NA
Y98A	0.4 ± 0.07	2.8 ± 0.1	7	NA	ND	NA
F124L	0.6 ± 0.03	11.1 ± 0.5	18.5	NA	ND	NA
I125A	NA	< 0.4	NA	NA	ND	NA
R128C	8.3 ± 2.9	24.4 ± 3.1	2.94	NA	ND	NA
I161G	0.95 ± 0.13	1.6 ± 0.05	1.7	NA	ND	NA
I161A	NA	ND	NA	NA	ND	NA
S71D, F124L	0.15 ± 0.02	6.5 ± 0.15	43.3	NA	ND	NA

NA, Not applicable; ND, not detected.

Table S4. Oligonucleotide primers for mutagenesis

Enzyme	Forward primer	Reverse primer
$VanXY_C$		
N8A	acaattgatcGCtaaaaaccatcc	atggtttttaGCgatcaattgtaatgtg
K9F	attgatcaatTTCaaccatccattgaaaaaaaatcaagagcc	atggatggttGAAattgatcaattgtaatgtg
D59S	tcgtctggtaAGtgggtatcgtacgg	cgtacgatacccaCTtaccagacgaatgtcc
Q67S	ggaaaaagaaTCgcgacgcttgtgggag	acaagcgtcgcGAttctttttccgtacg
Q67E	ggaaaaagaaGAgcgacgcttgtgggag	acaagcgtcgcTCttctttttccgtacg
L70E	acagcgacgcGAgtgggagtattctc	aatactcccacTCgcgtcgctgttctttttcc
E77L	ttctctaaaaCTaaacgggttagcttatacc	taacccgtttAGttttagagaatactccc
N78F	tctaaaagaaTTcgggttagcttatacc	aagctaacccgAAttcttttagagaatactcc
K84F	agcttataccTTCcaattcgttgctttgcc	caacgaattgGAAggtataagctaacccg
K84E	agcttataccGaacaattcgttgctttgcc	acgaattgttCggtataagctaacccg
A88D	caattcgttgAtttgccaggttgcagtg	acctggcaaaTcaacgaattgtttggtataagc
A88L	acaattcgttCTtttgccaggttgcagtgaacatc	acctggcaaaAGaacgaattgtttggtataagc
L89F	tcaaatcggtGCggccattgatgtagg	atcaatggccGCaccgatttgatgttcactgc
L99A	tcaaatcggtGCggccattgatgtagg	atcaatggccGCaccgatttgatgttcactgc
D111I	acaagaagatATtgatcttatctgccc	gataagatcaATatcttcttgtttctttagtcc
D112L	agaagatgatCTtcttatctgccctcattttcg	gcagataagaAGatcatcttcttgtttctttagtcc
L113F	gaagatgatgatTttatctgccctcattttcg	gagggcagataaAatcatcatcttcttg
L113E	agatgatgatGAGatctgccctcattttcg	gagggcagatCTCatcatcatcttcttgtttc
I114E	tgatgatcttGAGtgccctcattttcg	aatgagggcaCTCaagatcatcatcttcttg
C115R	gtatcagttatgCaccttggcattttcg	gaaaatgccaaggtGcataactgataccgg
C115E	tgatcttatcGAGcctcattttcgag	gaaaatgaggCTCgataagatcatcatcttc
G149L	agagatcaccCTatcagttatgaaccttggc	ataactgataAGggtgatctcttgtttatcttccg
G149E	gagatcaccgAGatcagttatgaaccttggc	cataactgatCTcggtgatctcttgtttatcttccg
G149F	agagatcaccTTatcagttatgaaccttggc	ataactgataAAggtgatctcttgtttatcttccg
I150G	gatcaccggtGGcagttatgaaccttggc	tcataactgCCaccggtgatctcttgtttatcttcc
I150A	gatcaccggtGCcagttatgaaccttggc	tcataactgGCaccggtgatctcttgtttatcttcc
E153A	gtatcagttatgCaccttggcattttcg	gaaaatgccaaggtGcataactgataccgg
Δ106–117	tggccattgatgtaggactatttcgagatagtgctgctgc	gcagcagcactatctcgaaatagtcctacatcaatggcca
Δ106–115	taggactaaagaaacaagaacctcattttcgagatagtgc	gcactatctcgaaaatgaggttcttgtttctttagtccta
$VanXY_G$		
S71D	atcgttcctgtaGAcggttatcgctcattagaag	agcgataaccgTCtacaggaacgatagagttacc
R74A	aagcggttatGCctcattagaagaacagacagcc	ttctaatgagGCataaccgcttacagg
R74H	agcggttatcActcattagaagaacagacagcc	ttctaatgagTgataaccgcttacaggaacg
Q79E	tcattagaagaaGagacagccatatatgacg	atatggctgtctCttcttctaatgagcg
Q79S	tcattagaagaaTCgacagccatatatgacg	atatggctgtcGAttcttctaatgagcg
I82A	acagacagccGCatatgacggctctctc	agccgtcatatGCggctgtctgttcttc
F94A	tggagaggatGCtacaagaaaatatgttgc	attttcttgtaGCatcctctccattatctttgag
Y98A	tacaagaaaaGCtgttgctctgccc	gcagagcaacaGCttttcttgtaaaatcctc
F124L	aaggatatagacCttatccgtcccgattttcc	cgggacggataaGgtctatatccttttttattcag
I125A	tatagactttGCccgtcccgattttccc	atcgggacggGCaaagtctatatcc
R128C	Not in database	
I161G	aataacagggGGttcacacgagccgtgg	gctcgtgtgaaCCccctgttatttcttctttatcc
I161A	aataacagggGCttcacacgagccgtgg	gctcgtgtgaaGCccctgttatttcttctttatcc

Lowercase letters indicate gene sequence. Uppercase letters indicate mutated sequence.